International Journal of Pavement Research and Technology
https://doi.org/10.1007/s42947-022-00255-x

社團法人中華鋪面工程學會
Chinese Society of Pavement Engineering

ORIGINAL RESEARCH PAPER

Improved Multi-layer Analysis of Pavement Response Using Neural Networks to Optimize Numerical Integration

Ahmed Abed[1] · **Nick Thom**[2] · **Ivan Campos-Guereta**[2] · **Gordon Airey**[2]

Received: 11 May 2022 / Revised: 7 November 2022 / Accepted: 9 November 2022

Abstract
This paper presents a new accurate method to compute the mechanical response of pavement structures using an Artificial Neural Network (ANN) model coupled with Multi-Layer Elastic Analysis (MLEA). The ANN model is used to improve the numerical integration of the response function used in the MLEA method. It requires four inputs: total pavement thickness, the diameter of the contact area, radial distance, and depth of the response point; and it was trained on one million hypothetical pavement structures. The developed method has been validated by a comparative analysis against boundary conditions, finite element analysis, and available MLEA solutions using various hypothetical pavement structures. The results demonstrate that the developed solution gives excellent response in the vicinity of the pavement surface together with a significant improvement in computational efficiency.

Keywords Pavement response · Multi-layer elastic analysis · Numerical integration · Artificial neural network

1 Introduction

The structural response of pavement layers to traffic loading plays a critical role in the design, analysis, and modelling of the pavement performance [1, 2]. Generally, pavement response modelling can be performed in two principal methods. The first is the Finite Element Analysis (FEA) [3–6], which can accurately model complex problems such as the mechanism of interaction between pavement surface and tyre [7–9]. The main drawback of this approach, however, is the computational time required to solve a single problem, it is, therefore, not considered suitable for routine pavement analysis and design problems. The second approach is Multi-Layer Elastic Analysis (MLEA). This analysis technique was first introduced by Burmister as a solution for two-layer systems [10], later extended to three-layer systems [11]. Over time, MLEA has expanded to allow analysis of greater numbers of layers and it has been implemented in widely used pavement analysis programmes such as JULEA [12], KenLayer [13], MnLayer [14], and others [15–17]; more details about these programmes are presented in Sect. 2.1. The advantage of this approach is that it provides a practically instant pavement response solution, which makes it suitable for routine pavement design, and also for probabilistic pavement design based on the Monte Carlo Simulation method, which requires repeated solving of pavement response [18–20]. This approach, however, has one main drawback which is the trade-off between response accuracy and computational speed near pavement surface [12, 13, 17].

Furthermore, there have been various advances in the analysis of pavement response such as analysis of multi-layer pavement structures with and viscoelastic media subjected under dynamic loads [21, 22] or impact loads [23, 24]. However, similar solutions may not be practical for everyday pavement analysis and design problems due to the advance knowledge required to implement these solutions. In fact, MLEA is still widely used by many pavement consultants and implemented in well-known pavement design methods such as the Mechanistic Empirical Pavement Design Guide [25] and the British design method [1] to solve pavement analysis and design problems. The accuracy of MLEA method, however, still requires further improvement especially in the vicinity of pavement surface,

✉ Ahmed Abed
abeda@aston.ac.uk

[1] Department of Civil Engineering, Aston University, Aston Triangle, Birmingham B4 7ET, UK

[2] Nottingham Transportation Engineering Centre, The University of Nottingham, University Park, Nottingham NG7 2RD, UK

Published online: 02 December 2022

as demonstrated in this work. Accordingly, the main aim of this study is to develop a flexible pavement response model capable of enhancing both precision and computational speed especially in the vicinity of the pavement surface where the pavement surface distress initiates. The new model involves application of MLEA together with a neural network model to enhance the numerical integration process involved in response calculation. The suggested solution has been coded in MATLAB, and the model results have been validated against boundary conditions at the pavement surface, FEA model, and available MLEA programmes. The validation process shows that the proposed model has enhanced response near the pavement surface with a more than doubling of computational efficiency compared to published data.

2 Methodology

2.1 MLEA

Considering a multi-layer linear elastic system with an axially symmetrical stress distribution subjected to a vertical load, such as the pavement structure shown in Fig. 1, stresses and displacements in polar coordinates at any point (*r, z*) can be calculated using the following equations [13]:

$$\sigma_z(r,z) = -mJ_0(m\rho)\Big(\big(A_i - C_i\big(1-2\mu_i - m\lambda\big)\big)e^{-m\left(\lambda_i-\lambda\right)} + \Big(B_i + D_i\big(1-2\mu_i - m\lambda\big)\Big)e^{-m\left(\lambda-\lambda_{i-1}\right)}\Big), \tag{1}$$

$$\sigma_r(r,z) = \left(mJ_0(m\rho) - \frac{J_1(m\rho)}{\rho}\right)\Big(\big(A_i + C_i(1+m\lambda)\big)e^{-m\left(\lambda_i-\lambda\right)} + \Big(B_i - D_i(1-m\lambda)\Big)e^{-m\left(\lambda-\lambda_{i-1}\right)}\Big) + 2\mu_i mJ_0(m\rho)\Big(C_i e^{-m\left(\lambda_i-\lambda\right)} - D_i e^{m\left(\lambda-\lambda_{i-1}\right)}\Big), \tag{2}$$

$$\sigma_t(r,z) = \frac{J_1(m\rho)}{\rho}\Big(\big(A_i + C_i(1+m\lambda)\big)e^{-m\left(\lambda_i-\lambda\right)} + \Big(B_i - D_i(1-m\lambda)\Big)e^{-m\left(\lambda-\lambda_{i-1}\right)}\Big) + 2\mu_i mJ_0(m\rho)\Big(C_i e^{-m\left(\lambda_i-\lambda\right)} - D_i e^{m\left(\lambda-\lambda_{i-1}\right)}\Big), \tag{3}$$

$$\tau_{rz}(r,z) = mJ_1(m\rho)\Big(\big(A_i + C_i\big(2\mu_i + m\lambda\big)\big)e^{-m\left(\lambda_i-\lambda\right)} - \big(B_i - D_i\big(2\mu_i - m\lambda\big)\big)e^{-m\left(\lambda-\lambda_{i-1}\right)}\Big), \tag{4}$$

$$w(r,z) = -\frac{1+\mu_i}{E_i}J_0(m\rho)\Big(\big(A_i - C_i\big(2-4\mu_i - m\lambda\big)\big)e^{-m\left(\lambda_i-\lambda\right)} - \big(B_i + D_i\big(2-4\mu_i - m\lambda\big)\big)\, e^{-m\left(\lambda-\lambda_{i-1}\right)}\Big), \tag{5}$$

$$u(r,z) = \frac{1+\mu_i}{E_i}J_1(m\rho)\Big(\big(A_i + C_i(1+m\lambda)\big)e^{-m\left(\lambda_i-\lambda\right)} + \big(B_i - D_i(1-m\lambda)\big)e^{-m\left(\lambda-\lambda_{i-1}\right)}\Big), \tag{6}$$

where r is radial distance from the load centre, z is the depth below the surface, σ_z, σ_r, and σ_t are vertical, radial, and tangential stresses respectively, τ_{rz} is shear stress, w and u are vertical and horizontal displacement, respectively, J_0 is a Bessel function of the first kind and order of 0, J_1 is a Bessel function of the first kind and order of 1, m is a parameter, A, B, C, and D are integration constants, μ is Poisson's ratio, E is modulus of elasticity, i is the layer number defined based on the depth of the analysis, ρ is r/H, λ is z/H, λ_i is the total thickness from the surface to the bottom of layer i divided by H which is the total thickness of the pavement from the surface to the top of subgrade. The assumptions of this system are that all layers are linear elastic, fully bonded, weightless, and the continuity condition applies for the vertical stress, shear stress and displacements at layer interfaces. Thus, these responses at the bottom of every layer are equal to those at the top of the next layer.

Equations 1 through 6, however, give stresses and displacements when the pavement is loaded with a concentrated vertical load of value $-mJ_0(m\rho)$. To convert this load into a distributed load over a circular area, the contact load must be accumulated over the contact area by performing a Hankel transform which takes the following form [13, 14]:

$$Q(m) = \int_0^{\alpha} q\rho J_0(m\rho)d\rho = \frac{q\alpha}{m}J_1(m\alpha), \tag{7}$$

where $\alpha = a/H$, a is the load radius, and q is the contact load. Accordingly, the pavement response due to a distributed load can be determined by introducing Eq. 7 into the response due to the concentrated load (Eqs. 1–6) and integrating the resulting functions with respect to m over the range 0-∞, as follows:

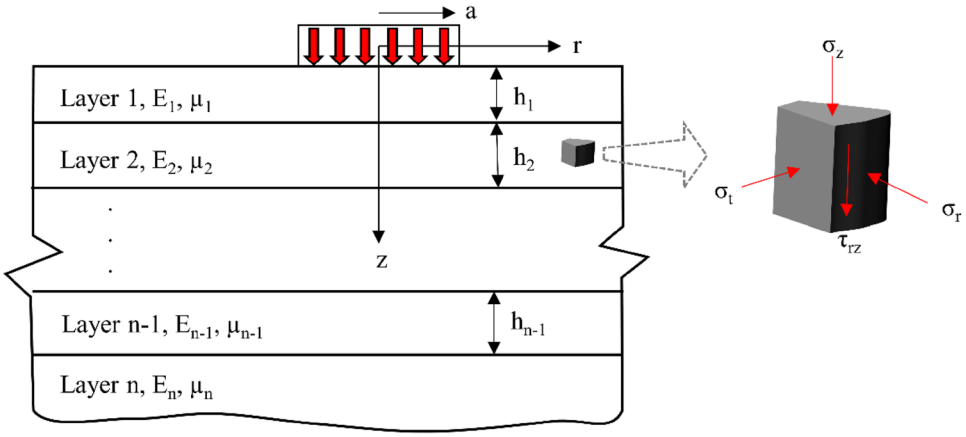

Fig. 1 A typical multi-layer pavement structure in polar coordinates

$$\begin{bmatrix} \sigma_Z \\ \sigma_R \\ \sigma_T \\ \tau_{RZ} \\ W \\ U \end{bmatrix} = \int_{m=0}^{\infty} \frac{q\alpha}{m} J_1(m\alpha). \begin{bmatrix} \sigma_z \\ \sigma_r \\ \sigma_t \\ \tau_{rz} \\ w \\ u \end{bmatrix} dm. \tag{8}$$

The capital subscripts in this equation are used to denote that the response is due to a distributed load q. The numerical solution of this system requires the determination of the integration constants A, B, C, and D for all layers and over all m values considered to reach a converged solution.

The integration constants can be determined from boundary and continuity conditions. Over the contact area, $z = 0$ and $r < a$, and the vertical stress $\sigma_{z1} = -mJ_0(m\rho)$; also, the shear stress at the pavement surface equals zero, thus $\tau_{rz}(z = 0) = 0$. At pavement layer interfaces, the vertical and shear stresses are equal based on the continuity condition. Similarly, the vertical and horizontal displacements at the interfaces are equal. Further, an infinite depth, $z = \infty$, the stresses should vanish, which means A_n and C_n must equal zero to meet this condition. To determine the integration constants, Huang [13] developed a method to calculate the constants of the last layer using the boundary conditions at the pavement surface then using these to calculate constants of the above layers one by one using the continuity conditions at the layer interfaces. Erlingsson and Ahmed [17] calculated the integration constants by arranging the equations resulting from the boundary and continuity conditions of a system of n layers into one master matrix, as follows:

$$[((n\ x\ 4) - 2), ((n\ x\ 4) - 2)]\ x \begin{bmatrix} A_1 \\ B_1 \\ C_1 \\ D_1 \\ . \\ . \\ . \\ A_{n-1} \\ B_{n-1} \\ C_{n-1} \\ D_{n-1} \\ B_n \\ D_n \end{bmatrix} = \begin{bmatrix} 1 \\ 0 \\ 0 \\ 0 \\ . \\ . \\ . \\ 0 \\ 0 \\ 0 \\ 0 \\ 0 \\ 0 \end{bmatrix}. \tag{9}$$

The detailed derivation of this equation can be found in the cited study. Equation 9 can be rewritten as [E] × {X} = {I} where matrix [E] is a matrix of linear equations derived from the boundary and continuity conditions; {X} is the unknown integration constant vector, and {I} is the input vector. It can be seen in Eq. 9 that A_n and C_n are not included; this is because their values are zero, which leads to the exclusion of two equations. This system of equations is a typical mathematical problem that can be solved by various methods; in this study, the Lower–Upper (LU) factorisation method was implemented. This method involves decomposing matrix [E] into lower and upper triangle matrices, which are used in forward and backward substitution processes to find the values of the unknowns. This method has been implemented in this study since it requires solving one matrix to determine the integration constants.

The determined integration constants can then be used in Eq. 8 to calculate pavement response at any point of interest. However, solving this equation is not straightforward since it involves solving a convolution integral of the product of two oscillating Bessel functions, which is a complicated mathematical problem. This problem has traditionally been solved by performing numerical integration in the range

between m equals zero and an m value that gives a converged solution allowing for certain integration error. This solution, however, can be computationally expensive, especially near pavement surface where the response function behaviour becomes complex and unpredictable. In this regard, different numerical integration techniques and 'tricks' have been suggested to improve the accuracy and convergence speed of the numerical integration process. Maina and Matsui [15] used a double exponential numerical integration formula in their work. They also implemented Richardson's extrapolation to improve the computational speed near the pavement surface. They demonstrated that this method improved the numerical integration accuracy, but they also stated that there was a problem in the response accuracy near the load edge. In KenLayer, Huang [13] used a four-point Gaussian formula to integrate numerically between the zeros of both Bessel functions (J0 and J1). And to improve integration accuracy, he subdivided the first cycle of J_0 into six intervals and the first cycle of J_1 into two intervals and integrated these using the four-point Gaussian formula. This approach obviously depends on the number of points taken between the zeros of the Bessel functions, and subdividing the first two cycles only into finer areas may lead to an error in the integration process as the entire response function should be integrated accurately. A similar approach was followed in MnLayer by Khazanovich and Wang [14] who also used a Gaussian formula to solve the numerical integration, but to improve the computation efficiency they calculated the integration constants at key m values then interpolated these to calculate them at required m values. Similarly, the monotonic part of the response function was also calculated at the key m values then interpolated that part to all m values. To further improve the response convergence speed near the surface, they calculated the response as a difference between two solutions; the first was for an elastic half space system having properties of the surface layer of the multi-layer system, the second was the difference in the response between the multi-layer system and the half space. They mentioned that this approached improved the convergence speed near the surface which is why it is implemented in MnLayer program. In JULEA and BISAR, Gaussian integration formulas are also employed [14, 17]. Cauwelaert [26] however, explained that the drawback of the Gaussian formula is that a different set of m values will be required for every combination of a and r. Therefore, he implemented the Newton–Coates integration method to provide as general and fast a solution as possible. Zhao et al. [16, 27] implemented two methods to improve the accuracy and speed of convergence near the pavement surface; the Lucas algorithm, which converts complicated oscillating behaviours such as the product of two Bessel functions into regular high and low-frequency components, and Richardson's extrapolation to speed up the integration process. They reported that this method improved

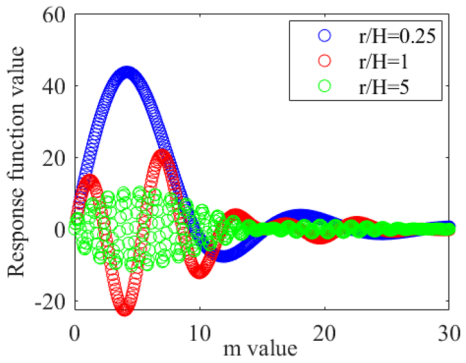

Fig. 2 r/H vs m

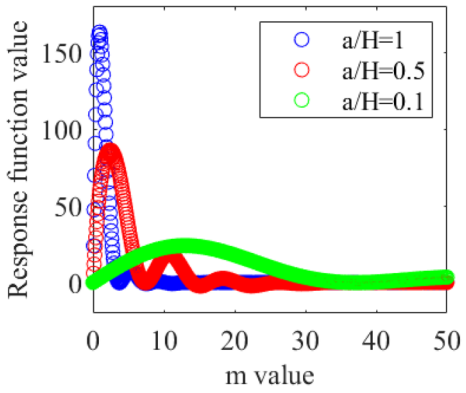

Fig. 3 a/H vs m

near-surface pavement response and computational speed in comparison with other pavement response programs such as KenLayer and BISAR.

2.2 Methodology of the Proposed Model

In most of the solutions reviewed, there was a common factor, which is the indetermination of the maximum Hankel parameter value that results in a converged solution. This means that the numerical integration process will continue slice by slice until the integration error reaches a predetermined tolerance, and this can slow down the integration process speed. In this study, however, it is suggested to predetermine the m value that gives a converged solution before attempting the numerical integration; this limit is designated as "*m max*". Therefore, the infinity term in Eq. 8 will be replaced by *m max* and the integration process will be between $m=0$ and $m=m\ max$. To achieve that, the relationship between the analysis inputs and *m max* was investigated. Equation 8 indicates that the response is a result of three functions, an exponential one which is a monotonic function depending on z/H and the integration constants, and two oscillating Bessel functions that depend on $m \times r/H$ and

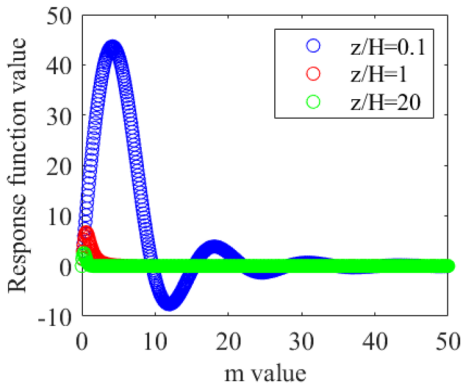

Fig. 4 *z/H* vs *m*

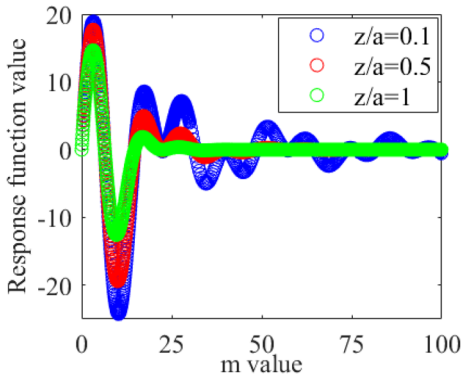

Fig. 5 *z/a* vs *m*

$m \times a/H$. Accordingly, the relationships between *m max* and *z, r, a* and *H* were analysed as presented in Figs. 2, 3, 4 and 5. From these figures the following trends can be observed:

1. The larger the value of *r/H*, the faster the function converges, as shown in Fig. 2; but this pattern is associated with significantly higher oscillations. Since *H* is usually assumed a constant value, then it can be concluded that the larger *r* becomes the lower *m max* will be but the more the function oscillates, which means it will be complex to integrate.
2. Figure 3 demonstrates that the smaller the contact radius, the larger the *m max* and the lower the oscillations.
3. The analysis depth is a critical parameter in the analysis process. Figures 4 and 5 indicate that the closer the analysis depth to the pavement surface, the more complex the response function will be. Although both Figures show that *z* is an important parameter, *z/H* did not show a critical effect on the results, as shown in Fig. 4. This figure indicates that small *z/H* leads to a higher oscillation, but the response function shape is still predictable with limited oscillations. On the other hand, despite it not being directly included in the analysis, the parameter *z/a* is found to be much more critical than *z/H* and it significantly affects both *m max* and the strength of oscillations, especially in the zone $z/a < 0.2$. Since *a* is usually a constant value, it can be concluded that the smaller the *z* the larger the *m max* and the greater the oscillations.

It can be seen that there are several conditions that can significantly affect *m max* and the extent of oscillations, and thus the complexity of the numerical integration process. To understand the underlaying relationship between *m max* and *z, r, a* and *H,* ANN method [28] was used. To apply this method, a lot of data are required to successfully train the model and detect the underlaying relationship between the inputs and the output. Accordingly, a MATLAB code was developed to collect the required data; the code firstly generates random input parameters with varying pavement structure thickness between 50 and 1500 mm, varying contact load radius between 50 and 170 mm, and random computational point coordinates with r between 0.1 and 10000 mm and z between 0.1 and 5000 mm. These conditions are sufficient to analyse all pavement structures and load geometries currently in practice. The randomness of the generated data was checked by running a Runs test at a level of significance

Fig. 6 ANN diagram

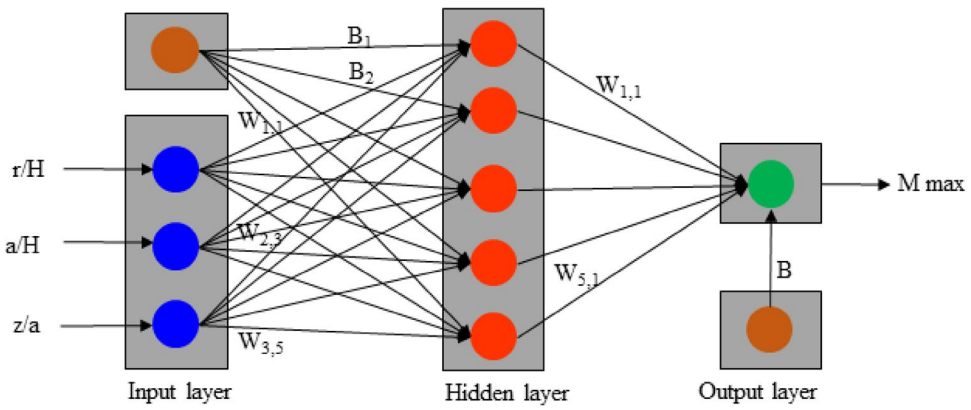

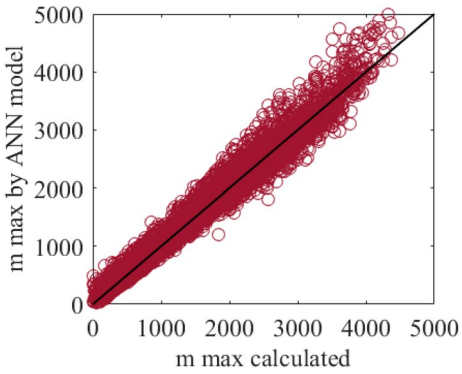

Fig. 7 Validation of the neural network model m max results

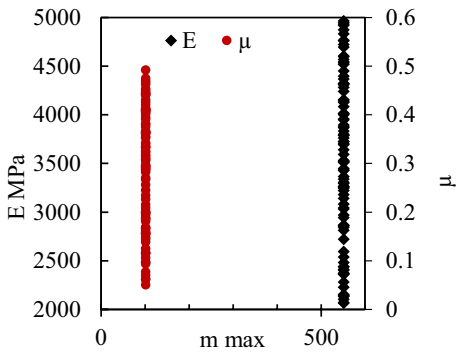

Fig. 8 An example of the relationship between E, μ and m max

of 5% [29]. Secondly, it calculates the numerical integration constants based on the properties of the generated structure. Third, it applies Eq. 8 which involves conducting numerical integration that stops when the predetermined numerical error is reached; lastly, it stores the *r/H, a/H, z/a* and *m max* parameters resulting from every iteration. By implementing this procedure, a total of one million combinations of datasets were collected, covering most possible multi-layer pavement structures. The collected data were used then to train the ANN model to drive the relationship between *m max* and the *r/H, a/H, z/a* parameters. Figure 6 shows the setup of the model which consists of an input layer, a hidden layer of five neurons, and an output layer. The number of neurons was optimised by a trial-and-error process; varying number of neurons between 3 and 10 was simultaneously tried and the corresponding R^2 values were registered, then the lowest number of neurons that gave the best fit was selected; this process showed that five neurons give the best fit for this model. The data were divided into three sections, 70% to derive the model, 15% to validate the model, and 15% to test the model. The ANN model was developed using the Levenberg–Marquardt backpropagation algorithm. The model results are shown in Fig. 7; these results show that there is a wide range of *m max*, approximately from 25 to ~ 5000. This depends on the analysed pavement geometry, applied load, and response point coordinates with respect to the load centre. Generally, the closer the response point to the load centre, the larger the *m max* value, and the closer the response point to the surface, the larger the extent of the oscillations. Accordingly, it can be concluded that the most difficult point to analyse is the one located at the surface and at the centre of the applied load, which is associated with large *m max* values and oscillations. However, Fig. 7 indicates that with these conditions, the ANN model tends to overestimate *m max* values. This can slightly increase the computational time, but it will not decrease the accuracy of the numerical integration. Moreover, it can be seen that the model can accurately predict *m max* with a coefficient of regression (R^2) of 0.996 for the various pavement geometries and load inputs included in the analysis. The R^2 values of the training, validation, and testing data were at least 0.996, which indicates the successfulness of the model in fitting the data. It must be stated here that the μ, q, and$E$ were not considered as inputs in the ANN model since varying these factors changes the amplitude of the response function rather than its extent or complexity. This means that changing the magnitudes of these factors would not change the value of *m max* as long as the geometry of the pavement under consideration and the load contact radius were kept the same. Figure 8 presents an example of the relationship between *E, μ* and *m max*; in this figure it can be noticed that changing the values of E and μ does not affect to the minimum integration boundary, m_max, to reach the predetermined tolerance in the numerical integration of Eq. 8.

Furthermore, it must be highlighted here that predetermining *m max* is critical for two purposes. First, it is used to determine an optimum *m max* for every computational point which can speed up the numerical integration process eventually the response at that point. Second, it is utilised to calculate optimised integration intervals over $m = 0$ and $m = max$. The latter significantly improves the accuracy of the integration process since it is performed over equal intervals in this case. It also improves the response computational efficiency in general by optimising the number of the integration constants, A_i, B_i, C_i, and D_i which must be calculated over all intervals of integration domain.

After determining *m max*, the next step is to evaluate the response function at a sufficient number of points between zero and *m max* in order to perform an accurate numerical integration. Bear in mind that the space between these points must be carefully estimated to capture the actual shape of the response. If the number of integration points is overestimated then the computational efficiency will decrease, but if it is underestimated then the accuracy of the numerical

integration will decrease. To overcome this issue, the number of zeros of Bessel functions is considered to optimise the required number of integration points. Since signs of the response function fluctuate from zero to zero over the x axis, and the zeros of the response function match with the zeros of the Bessel functions, then the number of points is calculated in this study as the number of zeros of Bessel functions of order zero that are smaller or equal to *m max* plus four points between each two successive zeros, and the number of zeros of Bessel functions of order one that are smaller or equal to *m max* plus four points between each two successive zeros. Calculating the number of evaluation points by this method has been found to satisfy the boundary conditions (σ_z equals applied load when $r<a$, and $\sigma_z=0$ when $r>a$); it has also been found satisfactory when the results of the current work were validated against other software, as discussed in the following sections.

Having determined the values of the Hankel parameter, it is now required to evaluate the response function at all of these points and fit a suitable function to match its behaviour. In this study, a cubic smoothing spline function embedded with Matlab has been utilised [30]. This function can provide a smooth fitting to a given dataset in a piecewise form; it was chosen due to its flexibility and superiority in fitting different complex patterns, which makes it suitable for the current application. Figure 9 presents an example of the fitting process results. This figure shows a dataset that was used in the fitting process denoted by the blue circles and the fitted spline. It also shows another set of validation data, calculated with a denser set of *m* values than the one used in the fitting data, which is taken to represent the exact solution of the response function. It can be seen that there is an excellent agreement between the fitted spline and the exact solution. Please note that the selected example in this figure demonstrates a complex response function shape with variable frequency and amplitude values. This means that the selected spline function gives excellent results even in complex situations such as the one shown in Fig. 9.

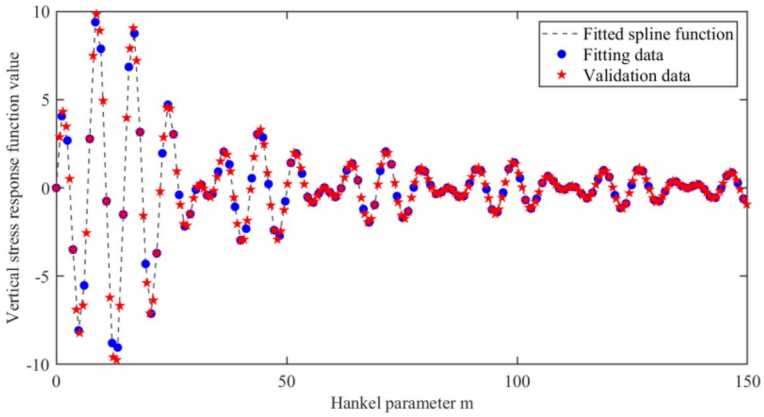

Fig. 9 An example of the matching between response functions calculated using fitted data and validation data

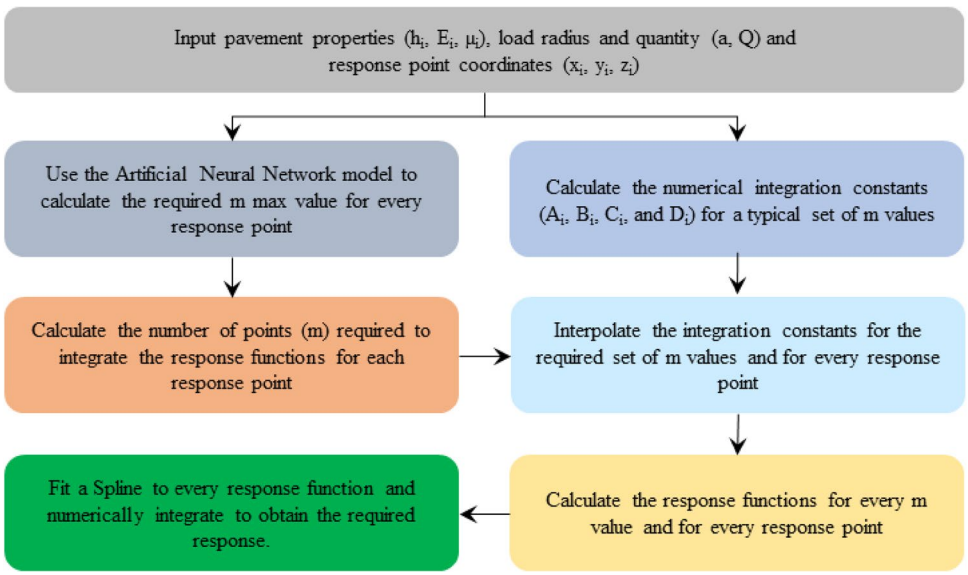

Fig. 10 Flowchart illustrating the logical steps of the proposed solution

The last point is to calculate the response by numerically integrating the fitted spline function between zero and *m max*; this has been performed by utilising the "integral" function embedded in MATLAB which involves using global adaptive quadrature integration. It is important to mention that calculating the integration constants at $m=0$ leads to a singularity of the matrix in Eq. 9. To overcome this issue, a very low initial *m* value of 1E-5 has been used in this study; this value has been used to calculate the integration constants and to evaluate response functions at $m \sim 0$. This approach has been found to be accurate and does not have any effect on the analysis results as shown in the next section.

To sum up, the suggested pavement response calculation process goes through the following main steps which are graphically explained in Fig. 10:

1. Calculate the integration constants for the pavement being analysed by solving Eq. 9. It must be mentioned here that this step requires solving the linear system for all Hankel parameters required to perform the numerical integration, which can be computationally expensive. To speed up this step, the concept described by Erlingsson and Ahmed [17] has been implemented. In this concept, the integration constants of all layers are calculated for a typical set of *m* values; a suitable model is then fitted to all constants of all layers; finally, the fitted model is used to interpolate the integration constants at all required *m* values, which are calculated after determining *m max* in step two. An example of this procedure is presented in Fig. 11. This Figure shows that the interpolated data fall exactly on the fitted spline which means the interpolation process is quite accurate. This step can decrease the computational time since the interpolation process is much faster than the process of solving the linear system. Also, the integration constants are functions of layer thickness and properties, which means one typical set of integration constants can be calculated for the multi-layer system being analysed; then for every *z* and *r* domain, a new set of integration constants is interpolated from the typical set of integration constants at the required *m* values for those particular coordinates.
2. Using pavement geometry, the coordinates of the required computational point, and the developed ANN model, the *m max* value is predicted. With this value, ρ, and α are then used to determine suitable *m* dataset between $m \sim 0$ and *m max* which will be used in the evaluation of the response functions.
3. Calculate the integration constants for all *m* values developed in step two by interpolation using the fitted model in step one.
4. Evaluate all response functions in Eq. 8 using the *m* values calculated in step two and the integration constants calculated in step three.
5. Fit a spline to every response function and numerically integrate to calculate the required response.

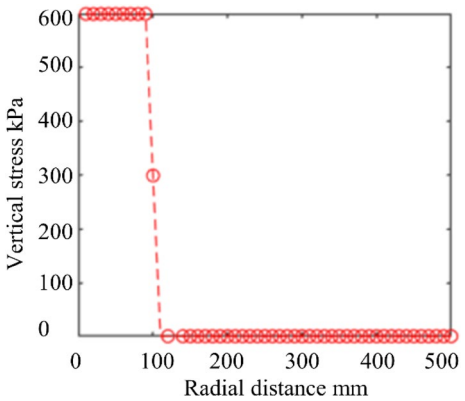

Fig. 12 σ_Z at surface of a two-layer system

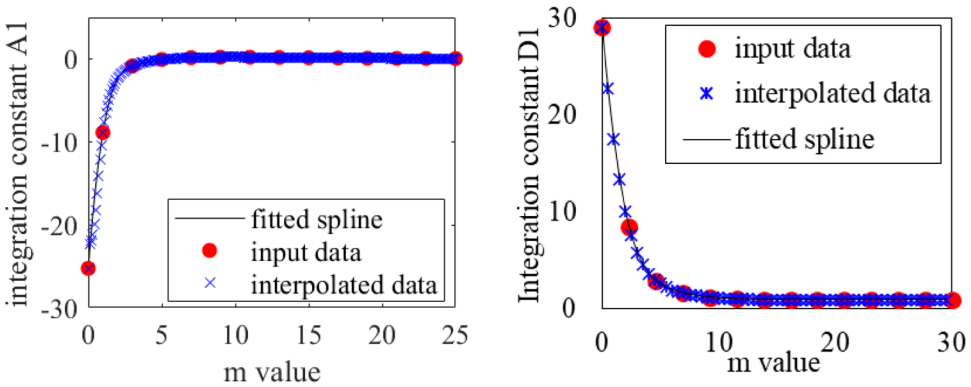

Fig. 11 Sample of the spline fitting and interpolation process results (Left: constant A results for layer 1 of a five-layer system. Right: constant D for layer 1 of a ten-layer system)

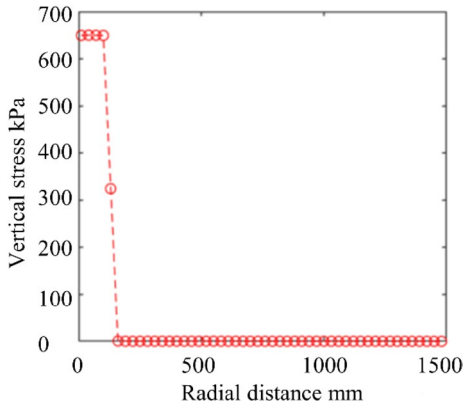

Fig. 13 σ_Z at surface of a three-layer system

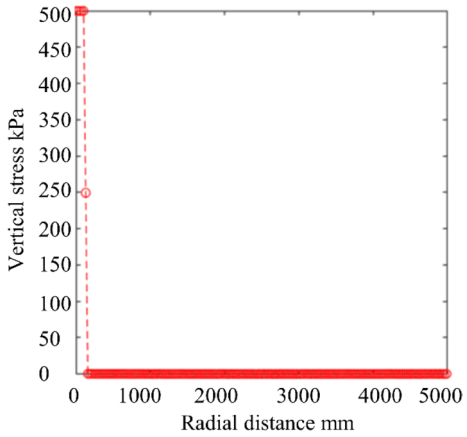

Fig. 14 σ_Z at surface of a four-layer system

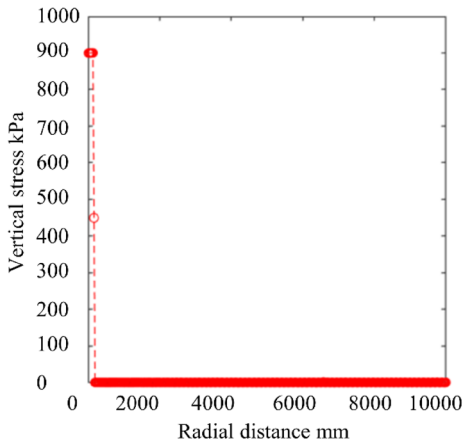

Fig. 15 σ_Z at surface of a five-layer system

Table 1 Properties of the pavement structures implemented in the validation process

System	2 layers	3 layers	4 layers	5 layers	6 layers
a mm	100	100	110	120	150
Q MPa	0.6	0.8	0.6	0.65	0.75
H mm	100	100	20	30	40
	inf	200	100	120	100
		inf	300	200	100
			inf	250	50
				inf	50
					Inf
E MPa	500	5000	10,000	7000	3500
	60	300	7000	10,000	8000
		100	200	500	500
			60	150	200
				50	100
					50

3 Results and Discussion

3.1 Validation Against Boundary Conditions

The solution derived in the previous sections was coded using MATLAB. To validate the developed code, two methods have been followed. Firstly, the vertical stress results of different multi-layer flexible pavements have been validated against boundary conditions at the surface ($\sigma_Z = q$ when $r < a$, and $\sigma_Z = 0$ when $r > a$). Figures 12, 13, 14 and 15 present the vertical stress results at the surface for two to six layer pavements with different loads and layer properties. It can be seen that the vertical stress equals the applied pressure under the contact area and equals zero outside the contact area, even when large radial distances are tested such as ten meters away from the load centre as shown in Fig. 15. Moreover, all of these figures show that at the edge of the contact area where $r = a$ and $\rho = \alpha$, the vertical stress equals half of that applied; this is because the integration result of the vertical stress response function equals q x 0.5 as explained by Zhao et al. [16]. Hence, the vertical stress at the pavement surface and the edge of the applied load can be considered as another validation of the analysis.

3.2 Validation of the Vertical Stress Near the Contact Area

In this section, a comparative analysis of the near-surface pavement response is presented. For this purpose, a 2D FEA model that was built using Abaqus CAE 2021 software, and three MLEA programs namely MnLayer, KenLayer and JULEA were selected to validate the results of the developed

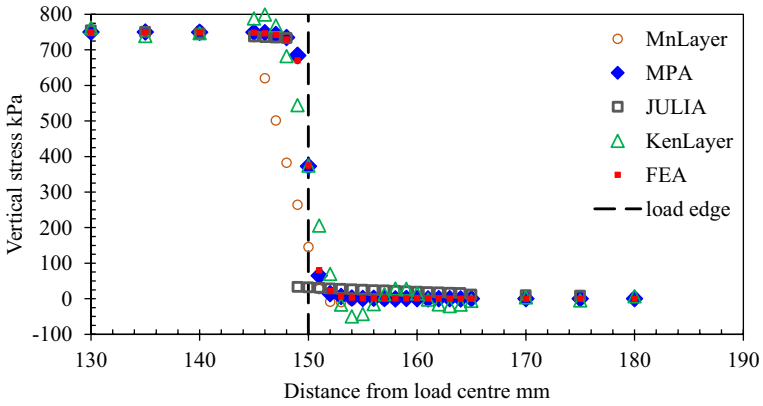

Fig. 16 Vertical stress profile at pavement surface and varying distances from load centre

Table 2 Statistical analysis results of the vertical stress response near the surface

Indicator	MPA	FEA	KenLayer	MnLayer	JULEA
RMSE	18.386	22.645	62.802	136.578	154.008
R^2	0.997	0.996	0.966	0.874	0.804

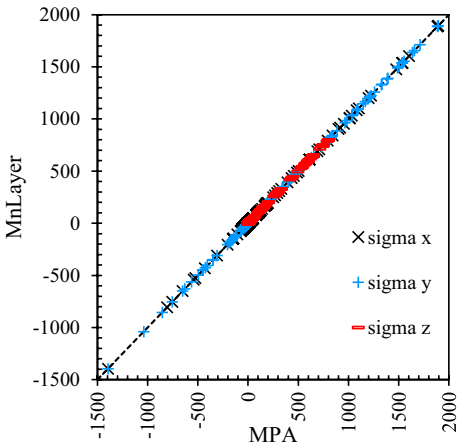

Fig. 17 Stress validation against MnLayer

solution. The FEA model compromised a geometry of 10 m width by 10m height in total; it was modelled using triangular linear elastic elements (3 nodes elements named CAX3). At the bottom and lateral boundaries, special infinite linear elastic elements has been included to extend the infinite half hemispace (4 nodes one-way infinite linear elastic elements named CINAX4). The mesh size of the model ranges from 0.5 mm on the load edge near the pavement surface, up to 0.5 m on the infinite half hemispace with a total of 112,655 to 245,959 elements for the varying pavement structures implemented in this study.

The six-layer pavement structure shown in Table 1 was used in this analysis since the exact solution for the vertical stress at the pavement surface can be determined from the boundary conditions, this stress was used in the analysis. Figure 16 presents the vertical stress results of all solutions at 1 mm depth below the surface. Results from the method described here are designated as "Multi-layer Pavement Analyser" (MPA) in the figure. This figure indicates that MnLayer resulted in a relative deviation from the boundary conditions around the load edge. KenLayer showed some increase in the vertical stress under the load next to the edge, followed by a decrease to about − 50 kPa at approximately 5 mm distance outside the load edge. Meanwhile JULEA zeroed the vertical stress at the load edge and even at 2 mm inside the edge, which constitutes to a critical error at this location. MPA, on the other hand, showed closer results to the boundary conditions with an excellent agreement with the FEA results. At the load edge, MPA and FEA obtained the exact result, which is half of the applied load as mentioned earlier. At 1 mm distance from either side the load edge, both solutions showed a minimal error of about 8% which can be attributed to the complexity of the numerical integration process at this location. At all other investigated points, MPA as well as FEA showed excellent agreement with the boundary conditions.

Furthermore, to quantify the computation error in MPA and the other programs, two indicators were investigated. The first indicator is the Root Mean Square Error (RMSE) which can be calculated as follows:

$$\mathrm{RMSE} = \sqrt{\sum_{i=1}^{n} (x_{1,i} - x_{2,i})^2 / n}, \tag{10}$$

where x_1 and x_2 refer to the first and second set of data, and n is the number of data points. The second is the coefficient of regression. The results are shown in Table 2; this table reports RMSE and R^2 results for MPA and the other programs as compared with the ideal response calculated from the boundary conditions. Based on 27 computational points, the RMSE of MPA is the lowest compared to the other programs. This means that its solution has the lowest

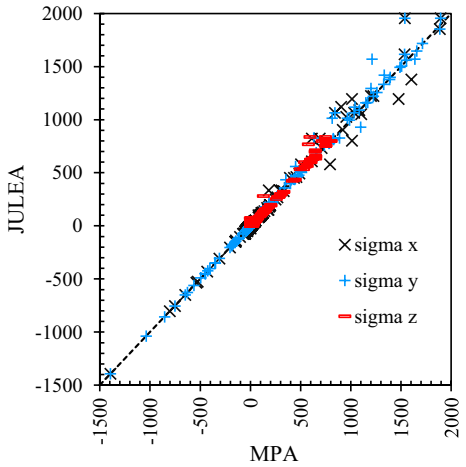

Fig. 18 Stress validation against JULEA

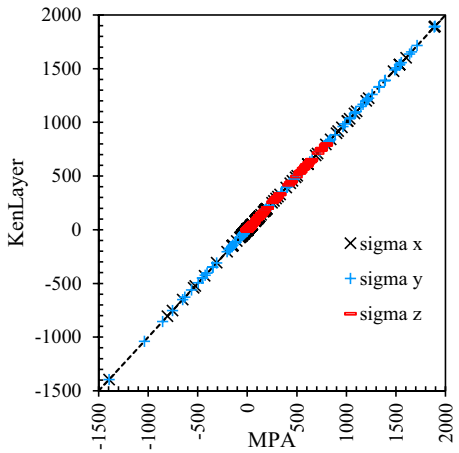

Fig. 19 Stress validation against KenLayer

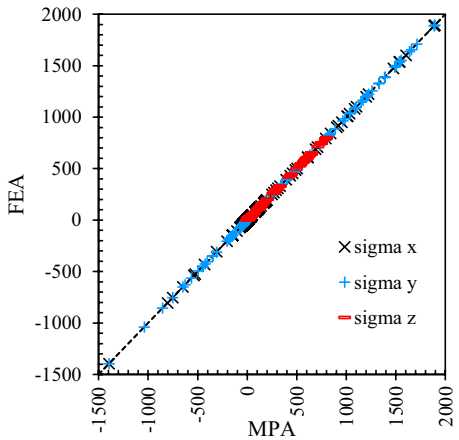

Fig. 20 Stress validation against FEA

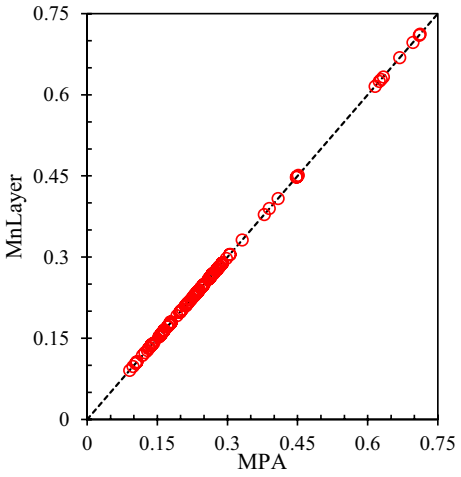

Fig. 21 *W* validation against MnLayer

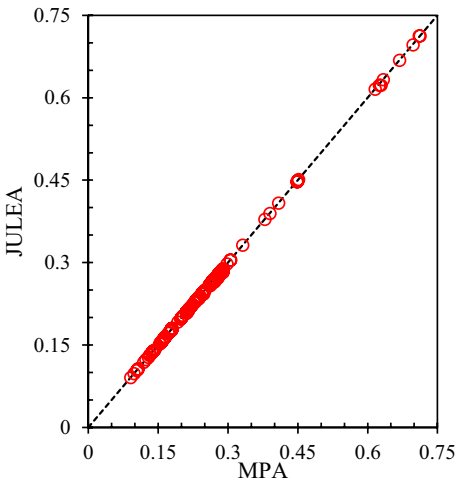

Fig. 22 *W* validation against JULEA

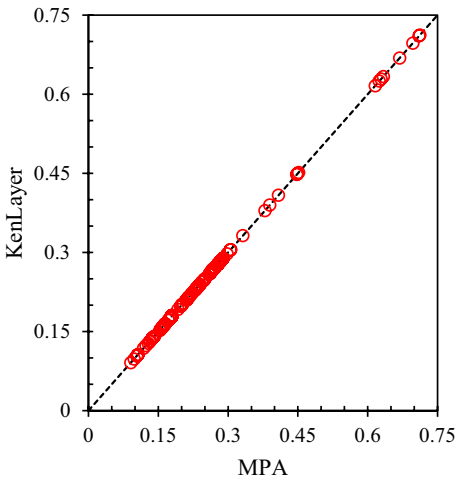

Fig. 23 *W* validation against KenLayer

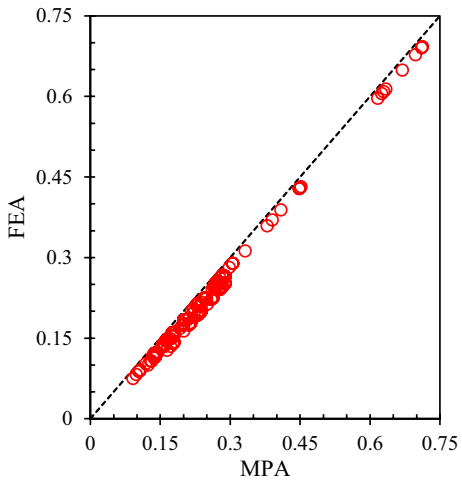

Fig. 24 *W* validation against FEA

Table 3 Statistical analysis of MPA response results with other programs

RMSE				
Solution	Sigma x	Sigma y	Sigma z	W
MnLayer	0.4888915	0.3794238	0.2119101	0.0000834
KenLayer	0.5173122	0.6543924	1.5390469	0.0007299
JULEA	55.7784196	50.3681348	29.2026109	0.0030642
FEA	1.2835471	1.5676654	0.3636570	0.0381466
R^2				
Solution	Sigma x	Sigma y	Sigma z	W
MnLayer	0.9999992	0.9999997	0.9999992	0.9999947
KenLayer	0.9999991	0.9999986	0.9999543	0.9999937
JULEA	0.9871832	0.9923115	0.9879420	0.9998649
FEA	0.9999961	0.9999946	0.9999975	0.9928050

error in terms of the vertical stress at the pavement surface. The Table also shows that R^2 is largest for MPA, which confirms the previous conclusion.

3.3 Validation of MPA Results Against Available Solutions

Apart from validating the vertical stress results against the boundary conditions at the pavement surface, the only way to validate pavement response is to compare the results against other approved pavement analysis programmes. To achieve that, the results of 2 to 6-layer pavements with varying thicknesses, contact loads, and contact radii were compared against the three other selected programs. The properties of the pavement structures are presented in Table 1. These structures are intended to cover a wide range of different possible pavement types; moduli are based on the authors' experience with back-calculated FWD measurements (at different temperatures). Since, strains are functions of stresses, then only stresses in x, y and z directions and vertical displacements were compared in this work. Figures 17, 18, 19 and 20 present comparative results of MPA against the other solutions for the x, y, and z stresses, respectively. Figures 21, 22, 23 and 24 present comparative results for vertical displacement. In general, these results show that there is an excellent agreement between MPA, MnLayer, FEA and KenLayer in all responses. There is also relatively good agreement between MPA and JULEA but to a lesser extent. Figures 17, 18, 19 and 20 show that most of the disagreements between MPA and JULEA are at points located near to the surface (i.e., high stresses). This agrees with observations from the literature that JULEA does not return an accurate response in the vicinity of the surface.

To further analyse these results and quantify the level of agreement between solutions, RMSE and R^2 were calculated, as shown in Table 3. This table indicates that there are small differences and high correlation between MPA, FEA, MnLayer, and KenLayer; it also indicates that there is a larger difference and poorer correlation between MPA and JULEA. Nevertheless, the absolute level of agreement is shown by fairly R^2 values amongst all solutions (>0.987).

3.4 Computational Efficiency of MPA

One of the important aspects of computer applications or algorithms is the processing speed or the "computational efficiency". In computer sciences, this topic is critical and can have various definitions. With respect to the current work, the computational efficiency is defined as the amount of time required to read the inputs, run the analysis, and return the results which are in this case pavement stresses, displacements and strains. The computational efficiency of the code was measured using the "tic-toc" function embedded in MATLAB, and it was then compared against other published computational time results [16]. In this study, the authors analysed a ten-layer system and measured the time required to calculate responses at twenty points near the pavement surface; the computational time for their code was 3.1 s. The authors also reported computational times for the same pavement system measured using two other programmes, BISAR and KenLayer, and the processing times for these programmes as reported by the authors were 6.4 and 5.4 s, respectively. In this work, the computation time for twenty points 1 mm below the surface of a ten-layer pavement structure and at different radial distances was 1.4 s as an average of twenty consecutive readings measured on a computer with Intel Core i3 CPU of 3.50 GHz. This constitutes a more than doubling of computational efficiency compared to the solution in [16] and around a four times

increase in efficiency against BISAR and KenLayer, yet with improved accuracy of results close the edge of the loaded area.

4 Conclusions

In this study, an innovative approach to calculate structural response of multi-layer pavements has been developed. The approach has involved developing an ANN model to predict the maximum value of Hankel parameter, *m max*, at which the numerical integration process of pavement response functions gives a converged solution. The main advantage of this solution is that it allows for the optimisation of the number of Hankel parameters and integration constants which significantly enhances the accuracy and computational efficiency of the response calculation process. The results of this approach have been validated against the boundary conditions, a FEA model and available MLEA solutions. Based on the results of this study, the following conclusions can be drawn:

1. Pavement geometry, contact radius, and coordinates of the response point have critical effects on the complexity and extent of the response function.
2. The response function was found to be very sensitive to the depth of the analysis, distance of the analysis, load radius, and total thickness of the pavement.
3. Comparisons of MPA results of various multilayer pavements against MnLayer, FEA, and KenLayer demonstrated excellent agreement associated with significant improvement in the response accuracy of MPA near the pavement surface, particularly at the edge of the loaded area.
4. Large m-max values are mostly required near the pavement surface. These values, however, may vary substantially depending on r/H, a/H, z/a parameters. Hence, the ANN model is used to optimise m-max based on the input parameters, which has significantly improved the numerical integration efficiency eventually the response calculation speed. This solution is therefore suitable for applications require quick response such instant back-calculation of pavement layer properties, or in pavement performance simulations that involve using the Monte Carlo simulation method which requires hundreds or thousands of iterations and pavement response calculations.
5. Multilayer elastic analysis represents a great deal of simplification to the actual behaviour of asphalt and unbound materials. In order to establish a relationship between the simplified model and the actual behaviour, one can consider calculating moduli of asphalt layers under certain temperatures and frequencies then consider the calculated moduli in the MLEA model. Similarly, equivalent moduli of the unbound layers can be derived under various humidity levels for instance, which can be used in the MLEA model. These measures could reduce the gap between the MLEA results and the actual response of the materials.
6. Future research will focus on expanding the developed approach to analyse viscoelastic material behaviour, pavement response to dynamic loading, and implementation in pavement management systems.

Acknowledgements The authors would like to acknowledge Professor Lev Khazanovich from the University of Pittsburgh for his support during the development of this work and for making MnLayer software available to the authors.

Funding The authors did not receive support from any organization for the submitted work.

Data Availability The data that support the findings of this study are openly available in: https://data.mendeley.com/datasets/hnt8yyr73v/draft?a=68f32728-b90c-4718-a7d1-75fc09d34b3e. Any further data required to reproduce the results of this study can be made available based on a reasonable request.

Declarations

Conflict of interest The authors declare that they have no competing interests.

References

1. Powell, W., Potter, J., Mayhew, H., and Nunn, M. (1984). The structural design of bituminous roads. Department of Transport, Transport and Road Research Laboratory, LR 1132 Monograph
2. ARA. (2004). Guide for mechanistic empirical design of new and rehabilitated pavement structures. ERES Consultants Division, Final Report 1–37A, Part 3 Chapter 3
3. Molavi Nojumi, M., Basavarajappa, M., Hashemian, L., & Bayat, A. (2022). Investigation of the impact of tire configurations on different pavement structures using finite element analysis. *International Journal of Pavement Research and Technology, 15*, 847–862.

4. Wang, H., Zhao, J., Hu, X., & Zhang, X. (2020). Flexible pavement response analysis under dynamic loading at different vehicle speeds and pavement surface roughness conditions. *Journal of Transportation Engineering, Part B: Pavements, 146*(3), 04020040.
5. Zhao, J., & Wang, H. (2020). Dynamic pavement response analysis under moving truck loads with random amplitudes. *Journal of Transportation Engineering, Part B: Pavements, 146*(2), 04020020.
6. Al-Qadi, I. L., Wang, H., Yoo, P. J., & Dessouky, S. H. (2008). Dynamic analysis and in situ validation of perpetual pavement response to vehicular loading. *Transportation Research Record, 2087*, 29–39.
7. Wang, H., & Al-Qadi, I. L. (2011). Evaluation of surface-related pavement damage due to tire braking. *Road Materials and Pavement Design, 11*, 101–121.
8. Shakiba, M., Gamez, A., Al-Qadi, I. L., & Little, D. N. (2016). Introducing realistic tire–pavement contact stresses into pavement analysis using nonlinear damage approach (PANDA). *International Journal of Pavement Engineering, 18*, 1027–1038.
9. Moazami, D., & Muniandy, R. (2021). Determination of rutting performance of asphalt pavements considering realistic tire-pavement contact area. *International Journal of Pavement Research and Technology, 14*, 764–770.
10. Burmister, D (1943). The theory of stresses and displacements in layered systems and applications of the design of airport runways. Board, Natl. Res. Counc.
11. Burmister, D. (1945). The general theory of stresses and displacements in layered systems I. *Journal of Applied Physics, 16*, 89–94.
12. Uzan, J. (1994). Advanced backcalculation techniques. Nondestructive Testing of Pavements and Backcalculation of Moduli: Second Volume. ASTM International
13. Huang, Y. (2004). Pavement analysis and design, 2nd edn. University of Kentucky: Pearson Prentice Hall
14. Khazanovich, L., & Wang, Q. (2007). MnLayer: high-performance layered elastic analysis program. *Transportation Research Record, 2037*(1), 63–75.
15. Maina, J., & Matsui, K. (2005). Elastic multi-layered analysis using DE-integration. *Publications of the Research institute for Mathematical Sciences, 41*, 853–867.
16. Zhao, Y., Zhou, C., Zeng, W., & Ni, Y. (2014). Accurate determination of near-surface responses of asphalt pavements. *Road Materials and Pavement Design, 16*, 186–199.
17. Erlingsson, S., & Ahmed, A. (2013). Fast layered elastic response program for the analysis of flexible pavement structures. *Road Materials and Pavement Design, 14*, 196–210.
18. Timm, D. H., & Newcomb, D. E. (2006). Perpetual pavement design for flexible pavements in the US. *International Journal of Pavement Engineering, 7*, 111–119.
19. Wu, Z., Yang, X., & Sun, X. (2017). Application of Monte Carlo filtering method in regional sensitivity analysis of AASHTOWare pavement ME design. *Journal of Traffic and Transportation Engineering (English Edition), 4*, 185–197.
20. Abed, A., Thom, N., & Neves, L. (2019). Probabilistic prediction of asphalt pavement performance. *Road Materials and Pavement Design, 20*, S247–S264.
21. Li, M., Wang, H., Xu, G., & Xie, P. (2017). Finite element modeling and parametric analysis of viscoelastic and nonlinear pavement responses under dynamic FWD loading. *Construction and Building Materials, 141*, 23–35.
22. Fan, H., Zhang, J., & Zheng, J. (2022). Dynamic response of a multi-layered pavement structure with subgrade modulus varying with depth subjected to a moving load. *Soil Dynamics and Earthquake Engineering, 160*, 107358.
23. Lee, H. S. (2013). Viscowave—a new solution for viscoelastic wave propagation of layered structures subjected to an impact load. *International Journal of Pavement Engineering, 15*, 542–557.
24. Quan, W., Ma, X., Si, C., Dong, Z., & Wang, T. (2021). Wave propagation approach for dynamic responses of transversely isotropic viscoelastic pavement under impact load. *Road Materials and Pavement Design, 23*, 2076–2097.
25. AASHTO (2008). Mechanistic-empirical pavement design guide: A manual of practice. American Association of State Highway and Transportation Officials. Washington, DC, USA.
26. Cauwelaert, F. V. (2003). *Pavement design and evaluation: The required mathematics and its applications*. Federation of the Belgian Cement Industry.
27. Zhao, Y., Wang, L., Chen, P., and Zeng, W. (2015). Determination of surface viscoelastic response of asphalt pavement. American Society of Civil Engineers. 141(1–8):04015031.
28. Yang, X., Guan, J., Ding, L., You, Z., Lee, V. C., Hasan, M. R. M., & Cheng, X. (2021). Research and applications of artificial neural network in pavement engineering: a state-of-the-art review. *Journal of Traffic and Transportation Engineering (English Edition), 8*(6), 1000–1021.
29. Corder, G. W., & Foreman, D. I. (2011). *Nonparametric statistics for non-statisticians*. John Wiley & Sons Inc.
30. MATLAB. (2020a) [Computer Software]. csaps: Cubic smoothing spline, The MathWorks Inc. https://www.mathworks.com/help/curvefit/csaps.html. Accessed Apr 2022.

Ahmed Abed is a research fellow at the department of civil engineering in Aston University; he has extensive experience in asphalt mix design and performance analysis, structural design and performance modelling of asphalt pavements. He is passionate about asphalt recycling, low energy asphalt, life cycle assessment of asphalt and asphalt pavements, and modelling of the surface deterioration of roads.

Nick Thom is a an Assistant Professor at the University of Nottingham. He has over 40 years of experience of highways design, construction and research, covering a wide breadth of topics. He specialises in pavement performance prediction of both surface skid resistance and structural deterioration, incorporating elements such as geogrid reinforcement and SAMIs.

Ivan Campos-Guereta MSc Civil Engineering at the Polytechnic University of Madrid, eMBA and PhD student in Civil Engineering; he has more than 24 years of experience as a consultant of civil engineering with experience in geotechnics, dams, roads and railways design, hydraulics and hydrological models, numerical modelling in general and programming. He has published some papers about hydraulic properties and numerical modelling of moisture content on roads and railway track layers, being this the topic of his recently submitted thesis at the University of Nottingham.

Gordon Airey is a Professor at the University of Nottingham with over 30 years of experience in pavement engineering materials. His main areas of expertise deal with the rheological characterisation of bitumen, bitumen-filler mastics and asphalt mixtures; the durability of asphalt materials; and the use of secondary materials, including crumb rubber and bio-binders.